Brett M. Noel, Steven B. Ouellette, Connor Navis, Laura Marholz, Tzu-Yi Yang, Vinh Nguyen, Sarah J. Parker, Zohar Sachs, Laurie L. Parker.

Multi-omic profiling of TKI resistant K562 cells suggests metabolic reprogramming to promote cell survival

Key Points:

- Alterations to metabolism are a common feature of target-mutation-independent resistance in CML cells across multiple clinically relevant TKIs.
- Carbonic anhydrase 1 (CA1) and α-synuclein (SNCA) are novel functional markers of metabolic reprogramming in TKI resistant CML cells.

Abstract

Resistance to chemotherapy can occur through a wide variety of mechanisms. Typically, resistance tyrosine kinase inhibitors (TKIs) is thought to arise from kinase mutations or signaling pathway reprogramming—however, "off-target" adaptations enabling survival in the presence of TKIs without resistant mutations are poorly understood. Previously, we established cell line resistance models for the three most commonly used TKIs in chronic myeloid leukemia treatment, and found that their resistance to cell death was not attributed entirely to failure of kinase inhibition. In the present study, we performed global, integrated proteomic and transcriptomic profiling of these cell lines to describe the mechanisms of resistance at the protein and gene expression level. We used whole transcriptome RNA sequencing and SWATH-based data-independent acquisition mass spectrometry (DIA-MS). This MS approach does not require

isotopic labels and provides quantitative measurements of proteins in a comprehensive, unbiased fashion: a significantly greater proportion of proteins are reliably quantified with this method, in comparison to traditional MS methods. The proteomic and transcriptional data were correlated to generate an integrated understanding of the gene expression and protein alterations associated with TKI resistance. We identified mechanisms of resistance that were unique to each TKI. Additionally, we defined mechanisms of resistance that were common to all TKIs tested. Resistance to all of the TKIs was associated with the oxidative stress responses, hypoxia signatures, and apparent metabolic reprogramming of the cells. Metabolite profiling and glucose-dependence experiments showed that the resistant cells relied on glycolysis (particularly through the pentose phosphate pathway) more heavily than the sensitive cells, which supported the idea that metabolism alterations were associated with resistant cell survival. These experiments are the first to report a global, integrated proteomic and transcriptomic analysis of TKI resistance. These data suggest that targeting metabolic pathways along with TKI treatment may overcome pan-TKI resistance.

Introduction

CML is characterized by translocation of chromosomes 9 and 22 to form the Philadelphia chromosome, which generates a fusion between the breakpoint cluster region (*BCR*) gene and the *ABL1* gene. The product of this fusion is the Bcr-Abl protein, in which several of the autoregulatory features of the Abl protein tyrosine kinase are disrupted, leading to its constitutive activity. Tyrosine kinase inhibitors (TKIs) inhibit Abl activity and are the major treatment modality for chronic myelogenous leukemia (CML). The first blockbuster TKI, imatinib, was introduced in the 1990s and provided a transformational improvement in outcomes for CML

patients, increasing the five year survival rate from ~45% to >80% and launching a new paradigm for molecularly targeted cancer therapy that has resulted in development of additional inhibitors for second, third, and further lines of therapy in CML and other cancers.[1]

However, and perhaps inevitably, resistance or failure to respond has emerged as a significant clinical problem affecting about 33% of CML patients and leading to disease progression. Increasing clinical evidence is accumulating that sequential treatment with first, then second, then third line kinase inhibitors (starting with imatinib) does not result in better survival, and in fact, increases the risk of multidrug resistance.[2] Suboptimal response to imatinib is associated with lack of Bcr-Abl inhibition by 1 month,[3] and is observed at 18 months in up to 40% of CML patients.[4] Second line dasatinib and/or nilotinib is effective for about half of imatinib-resistant patients, but third line TKIs do little to improve the long term outlook: patients who fail to respond to two TKIs are unlikely to achieve durable responses with a third TKI.[5,6] *ABL* mutation (e.g. T315I in *BCR-ABL*) is a clinically significant mechanism of early first line response failure, with incidence between 40-90% (depending on definitions and detection methods),[4] however second line failure is mutation-independent in 40-70% of cases.[5,6]

In general, mutation-independent resistance can arise from several potential mechanisms, including amplification of the target protein (through copy number increases, increased transcription or translation, and/or decreased turnover), increased drug efflux or decreased drug influx through transporter proteins, or alteration in dependence on other signaling pathways (often termed "kinome reprogramming"[7,8]). Increasing evidence is also accumulating that metabolic reprogramming (relying more heavily on glycolysis as a response to oxidative stress) can enable cancer cells to adapt to stress (including chemotherapeutic stress) and survive in the presence of apoptotic signaling.[9] Despite a breadth of literature on the role of metabolic

reprogramming in solid tumors and other leukemias and lymphomas,[9,10] there has been less exploration of the potential for metabolic reprogramming to influence sensitivity of CML cells to kinase inhibitors. Evidence for imatinib resistance dependent on metabolic reprogramming through HIF1α has been reported,[11] however no global evaluation of markers or comparisons to resistance to other TKIs has been performed so far.

Because CML patients that fail two TKIs face dismal outcomes, it is imperative to find new avenues for therapy. Understanding the cooperating molecular pathways that allow CML cells to survive TKI treatment could be instrumental in guiding therapy for these patients. Several studies have examined mechanisms of TKI resistance in CML, typically for one or at most two TKIs, using either RNA sequencing (RNAseq) or protein analyses. However, without complex algorithmic normalization, there is often surprisingly little correlation between transcript and protein levels in the cell.[12] While gene expression data is highly informative, the absence of protein-level data in TKI resistance severely limits our ability to understand the role of kinome and metabolic reprogramming. To our knowledge, combined comparisons of RNA and protein resistance profiles for all three of commonly used TKIs have not previously been performed. In this report, we sought to define these relationships to obtain a comprehensive characterization of resistance common to multiple TKIs. We performed transcriptomic and proteomic analyses of the TKI-sensitive human CML cell line K562 and three TKI-resistant derivatives developed in our laboratory: K562-IR (imatinib resistant), K562-NR (nilotinib resistant), and K562-DR (dasatinib resistant).[13] These cell lines were generated by continuous, increasing dosage exposure to kinase inhibitors over >90 days until a resistant population was generated. Quantitative, whole transcriptome RNAseq and data-independent acquisition (DIA) SWATH-MS datasets were generated. SWATH-MS combines the best features of both narrowly targeted (e.g. multiple

reaction monitoring, MRM) and broad, unbiased protein profiling mass spectrometry methods, which enabled label-free quantitative analysis of relative protein abundance on a global proteome level. Each dataset was analyzed to identify differential gene and protein abundance between cells lines. An integrated analysis of the transcriptomic and proteomic data revealed common features of resistance to these kinase inhibitors: downregulation of Myc targets, engagement of hypoxia-related signaling, alteration of post-transcriptional/translational regulation, and metabolic reprogramming. Labeled glucose feeding experiments confirmed differences in metabolism for the resistant vs. sensitive cells, including increased glycolysis and shunting to the pentose phosphate pathway. Phenotypic experiments testing the ability of the cells to grow in galactose vs. glucose provided evidence that the resistant cells were more dependent on glycolysis as their major metabolic pathway than the sensitive cells, which were able to adapt and grow using other energy sources e.g. OXPHOS. Overall, these data suggest that targeting metabolic adaptation may provide valuable targets for avoiding and/or overcoming target mutation-independent resistance in CML.

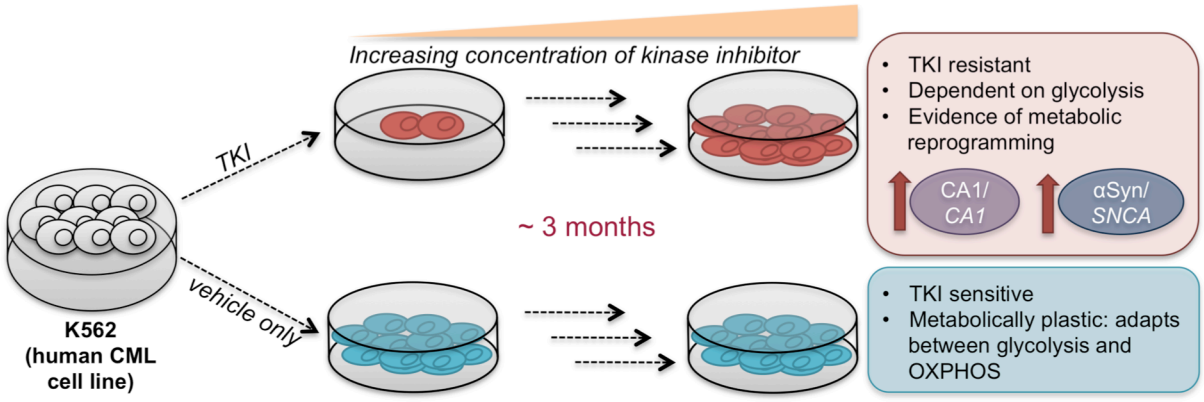

Figure 1. Developed resistance of a CML cell line to three different clinically-relevant tyrosine kinase inhibitors (TKIs) is associated with metabolic reprogramming that alters dependence on glycolysis and metabolic plasticity. Carbonic anhydrase 1 (CA1/*CA1*) and α-synuclein (αSyn/*SNCA*) protein and mRNA levels emerged as a potential mechanistic biomarker signature for this type of metabolic reprogramming in K562 CML cells.

Materials and Methods

Cell culture

K562 cells were purchased from ATCC. Imatinib resistant (IR), nilotinib resistant (NR), and dasatinib resistant (DR) K562 cells were generated in the lab as described in our previous report of these cells[13] by culturing K562 cells in the presence of low, but increasing concentrations of TKIs for 90 days, followed by a constant concentration from then on (1μM imatinib or 10nM nilotinib or 1nM dasatinib supplemented IMDM with 10% fetal bovine serum and 1% penicillium/streptomycin). Cells were grown to 7.5 x 10^5 cells/mL and split into two equal parts for RNAseq analysis and SWATH-MS.

RNA sequencing sample preparation and analysis

Cellular RNA was extracted in triplicate for each sample with the RNEasy kit (Qiagen) following manufacturer's instructions. RNA concentration was measured, diluted to 100ng/μL, and submitted to the University of Minnesota Genomics Center (UMGC) for paired-end RNA sequencing. Twelve barcoded TruSeq RNA v2 libraries (four cell lines, triplicate RNA samples) were created from the samples and combined for sequencing on a HiSeq 2500 using rapid mode with 50bp reads, for a total of ~5-7 million reads per sample. Data format was converted to FASTQsanger and mapped to human reference genome (hg19_canonical) using TopHat2 on the Galaxy platform installed on the high performance cluster in the Minnesota Supercomputing Institute (MSI) at the University of Minnesota. Differential expression testing between the wild type K562 cells and K562-IR, K562-NR, and K562-DR cells, respectively, was computed using both Cuffdiff (via comparison of FKPM values generated using CuffQuant), a transcript

computation program available as a package through Cufflinks,[14] and edgeR (using raw read counts from featureCounts). Subsequently, fusion transcripts were detected using DeFuse,[15] a software package used to detect fusion transcripts from paired-end RNA-seq data.

Proteomics sample preparation and mass spectrometry analysis

Cells were washed three times with ice-cold PBS and re-suspended in lysis buffer (50mM ammonium bicarbonate pH 7.0, 4mM EDTA, Roche phosphatase inhibitors cocktail) and immediately incubated at 95°C for five minutes to seize all enzymatic activities. Subsequently, cells were sonicated for 30 minutes in a water bath and the insoluble fraction was separated from the cell lysate by centrifugation at 1.5 x 10^3 RPM for 20 minutes at 4°C. Each sample was reduced (20mM dithiothreitol for 1 hour at 60°C), and alkylated (40mM iodoacetamide for 30 minutes at room temperature in dark.) Reactions were quenched by adding dithiothreitol to a final concentration of 10mM. The samples were then trypsin digested overnight at 37°C at a ratio of 1:50 (w/w). Subsequently, samples were cleaned up using MCX-type stage tips[16] and re-suspended in 90% water/10% acetonitrile/0.1% formic acid to a final concentration of 0.16 mg/mL. Samples (800ng tryptic digest) were separated on a LC/MS system which included an Eksigent NanoLC 400 system and an AB SCIEX 5600 TripleTOF mass spectrometer. Samples were analyzed using a "trap and elute" configuration on the Eksigent nanoFlex system. Samples were loaded at 2 µL/min for 10 minutes onto a trap column (200 µm x 0.5 mm ChromXP C18-CL chip column) and resolved on an analytical column (75 µm x 15 cm ChromXP C18-CL 3µm.) Mobile phase of the liquid chromatography systems are: 0.1% (v/v) formic acid in LCMS grade water (solvent A) and 0.1% (v/v) formic acid in LCMS grade acetonitrile (solvent B). The LC method was over 90 min with a gradient from 5% to 35% solvent B at a flow rate of 300

nL/min. The mass spectrometer was set to acquire SWATH data (i.e. data independent acquisition, DIA).[17] In a cycle time of about 1.8 sec, one survey scan and thirty-four 26 Da SWATH scans were performed. These 26 Da-wide scan events sequentially cover the mass range of 400 – 1250 Da, with a 1 Da for the window overlap. The collision energy for each SWATH scan was increased sequentially to better fragment peptide ions.

Metabolite profiling

A total of 21 million of both the wild type (WT) and imatinib-resistant (IR) K562 cells were diluted to 800,000 cells per mL in glucose-free RPMI 1640 medium (Thermo Fisher Scientific) with 5% fetal bovine serum and 1% penicillin-streptomycin, which was supplemented with 25 mM 6-^{13}C labeled D-glucose (Cambridge Isotope Laboratories). The cells were subjected to this treatment for 12.5 h, and then the metabolites were extracted in triplicate (7 million cells per replicate) from both the WT and IR lines according to instructions and with materials provided by Human Metabolome Technologies, Inc. (HMT). Briefly, the cells were first centrifuged down at 1,200 rpm for 5 min at room temperature and the culture medium was removed by aspiration. 10 mL of a 5% (w/w) solution of D-mannitol in Milli-Q water was added to each sample and the pellets were resuspended and centrifuged as before. The supernatant was removed by aspiration and then 800 µL of LC-MS grade methanol was added to each cell pellet and vortexed for 30 seconds. Then, 550 µL of an internal standard solution (provided by HMT and diluted 1:1000 in Milli-Q water) was added to each sample and vortexed for 30 seconds. A total of 1000 µL of this mixture was transferred to microtubes which were centrifuged at 2,300 g for 5 min at 4° C. Next, 350 µL of the supernatant was transferred to pre-washed centrifugal filter units in duplicate (due to volume constraints of the filter units) and centrifuged at 9,100 g for 3 h at 4° C. The filtered

solutions were then evaporated to dryness using a SpeedVac. The samples were then stored at -80° C until they were shipped to HMT for analysis. The metabolite profiling measurements (HMT's "F-Scope" service) were performed on each of the 6 samples (3 WT and 3 IR) using capillary electrophoresis time-of-flight mass spectrometry (CE-TOFMS).

Results

Whole transcriptome analysis: Resistance is mediated by pathway alterations and not *BCR-ABL1* gatekeeper mutations

In order to detect differences in gene expression associated with TKI resistance, we performed whole transcriptome RNA sequencing analysis on parental K562 human chronic myeloid leukemia cells and three drug-resistant derivatives, K562-IR (imatinib-resistant), K562-NR (nilotinib-resistant), and K562-DR (dasatinib-resistant). Sequencing was performed for three replicate samples from each cell line. Fusion transcripts were detected using the DeFuse package[15] in Galaxy. The *BCR-ABL1* t(9;22) fusion transcript was validated in each cell line, and several other fusions were also observed (including e.g. the known fusion *NUP214-XKR3* t(9;22)[18,19]) (Supplementary Table S1). To examine the *BCR-ABL1* transcripts for potential drug-resistant point mutations, a custom version of the human hg19 genome was built to incorporate the *BCR-ABL1* fusion gene, map the specific fusion transcripts and identify whether point mutations in the gatekeeper residue were associated with inhibitor resistance. Using IGV Browser (Broad Institute) to view the mapped reads of each TKI-resistant derivative against this custom genome, we did not identify any point mutations that were significantly different in the resistant vs. the sensitive cell lines. In particular, the gatekeeper residue T315 was not modified,

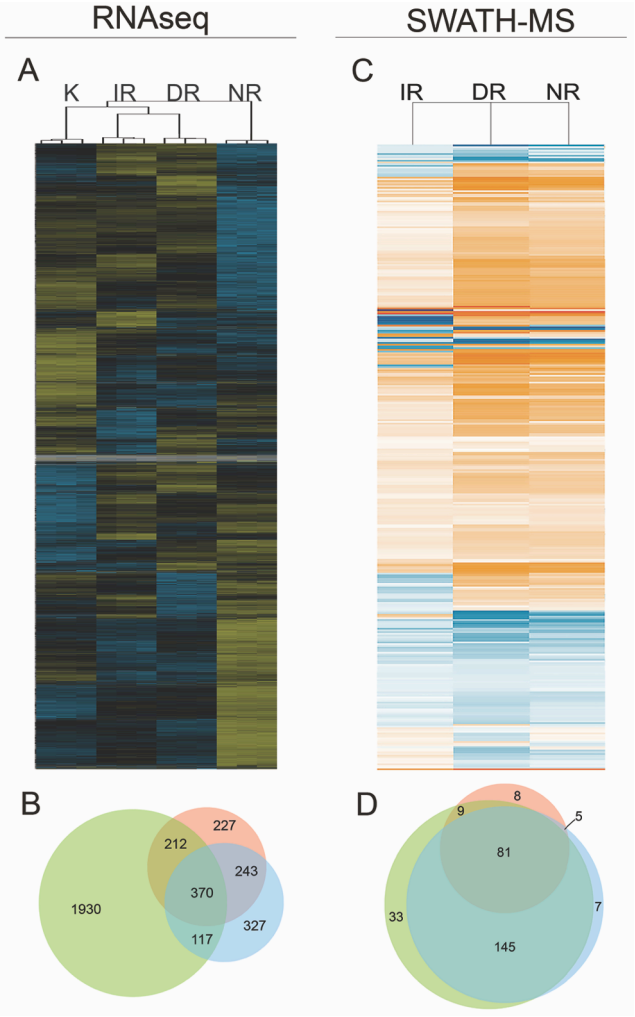

Figure 2. Differential gene and protein expression summary. A) Heatmap of expression levels (FKPM) for all genes observed by RNAseq. K = control K562 cells, IR = imatinib-resistant, DR = dasatinib-resistant, NR = nilotinib resistant. B) Venn diagram showing number of overlapping and unique differential gene expression (calculated as log2 fold change) observed in RNAseq data from the different TKI resistant cell lines relative to the control K562 cells. C) Heatmap for all proteins detected in resistant cells with log2 fold change >1 and OneOmics confidence of >75% for differential expression relative to control K562 cells. IR = imatinib resistant, DR = dasatinib resistant, NR = nilotinib resistant. D) Venn diagram showing number of overlapping and unique proteins observed as differentially expressed (by log2 fold change) in the SWATH-MS data for the TKI resistant cell lines relative to the control K562 cells.

strongly suggesting that gatekeeper mutations were not contributing to drug resistance in these cell line models (Supporting information Fig S1).

We compared the differentially expressed genes of each TKI resistant cell line relative to the parental, sensitive cell line (Supplementary Tables S2-S5). Each TKI resistant cell line differentially expressed a unique set of genes (227 for the imatinib-resistant cells, 327 for the dasatinib-resistant cells, and 1930 for the nilotinib-resistant cells). However, we also found 370 genes that were differentially expressed in common across all three TKI resistant cell lines (Fig. 2A,B) Of these, 117 were downregulated and 253 were upregulated by $\log_2$ fold-change of at least at least -1 or 1, respectively in each TKI resistant sample, with 97% concordance of $\log_2$ fold-change direction per transcript across all three cell lines (Table S7). Because we were most interested in the mechanisms

that might be common targets in TKI resistance, we focused on genes that were commonly differentially expressed in all the drug resistant cell lines. Several of these transcripts have previously been identified as associated with TKI resistance, including MDR1/ABCB1, CD36, CD44, β-catenin, FYN, and AXL (Fig. S2, S5), indicating that our models were comparable to others developed in the literature.[20-24] Additionally, Ingenuity Pathway Analysis and Gene Set Enrichment Analysis (Fig. S3 and S4) identified alterations to Myc programming, activation of HIF1α pathways, and oxidative stress processes in the TKI resistant cells. These represent novel pathways associated with TKI resistance. Interestingly, all of these alterations involve metabolic changes. [25, 26]

Quantitative protein level profiling: Proteome-level pathway alterations are consistent with gene expression-level pathway observations

To define mechanisms of TKI-resistance at the protein level, we also performed quantitative proteomics (on the same set of samples as for RNAseq) using SWATH-MS data on a 5600+ TripleTOF® instrument (SCIEX). Protein extracts were analyzed using a fixed window (25 Da) in SWATH mode, which allowed for recording of fragment ion spectra from all detectable peptides in the samples and enabled unbiased label-free quantitative comparisons of the proteome (Tables S8 and S9). These analyses detected a set of uniquely differentially expressed proteins in each TKI-resistant cell line relative to the parental control (8, 7, and 33 for the imatinib-resistant, dasatinib-resistant and nilotinib-resistant cell lines, respectively). 81 proteins were differentially expressed in common amongst the three drug resistant cell lines compared to the sensitive parental control cells, with 70% concordance of $\log_2$ fold-change direction (Figure

2C,D). Ingenuity Pathway Analysis (Figure S4) supported the gene expression analyses that oxidative stress and metabolic processes were different (relative to the TKI-sensitive cells) in all three of the TKI resistant cell lines. As discussed below, the protein-level data provided important information about whether transcripts observed in the RNAseq experiment actually gave rise to altered levels of proteins, and illustrate how even with substantial mRNA $\log_2$ fold-change concordance, proteins alterations were more variable between the different cell lines.

Combined analysis: Relationships between gene expression and protein level patterns in kinase inhibitor resistance

We performed an analysis to integrated transcriptomic and proteomic datasets to examine the relationships between mRNA and protein alterations in TKI-resistant cells. RNAseq and SWATH-MS datasets were aligned using the OneOmics MultiOmics tool to identify transcript observations that had corresponding protein observations (Supplementary Table S10). 588 were matched in common across all cell lines with sufficient confidence at both the mRNA and protein levels. The relationship between mRNA and protein fold changes was examined for transcripts and their associated proteins that were observed in both. Overall, there was a moderate, but statistically significant, correlation between mRNA and protein level fold changes in each resistant cell line relative to the control (Fig. 3A). In general, the magnitude of differential expression for proteins varied more widely than it did for mRNAs between the TKI sensitive vs. the TKI resistant cells: in many cases for a gene, the protein levels exceeded the fold change cutoff ($\log_2$FC >1 or $\log_2$FC<-1) but the respective mRNA levels did not ($\log_2$FC = -1 to 1). These findings are consistent with the enriched GO annotations observed for the

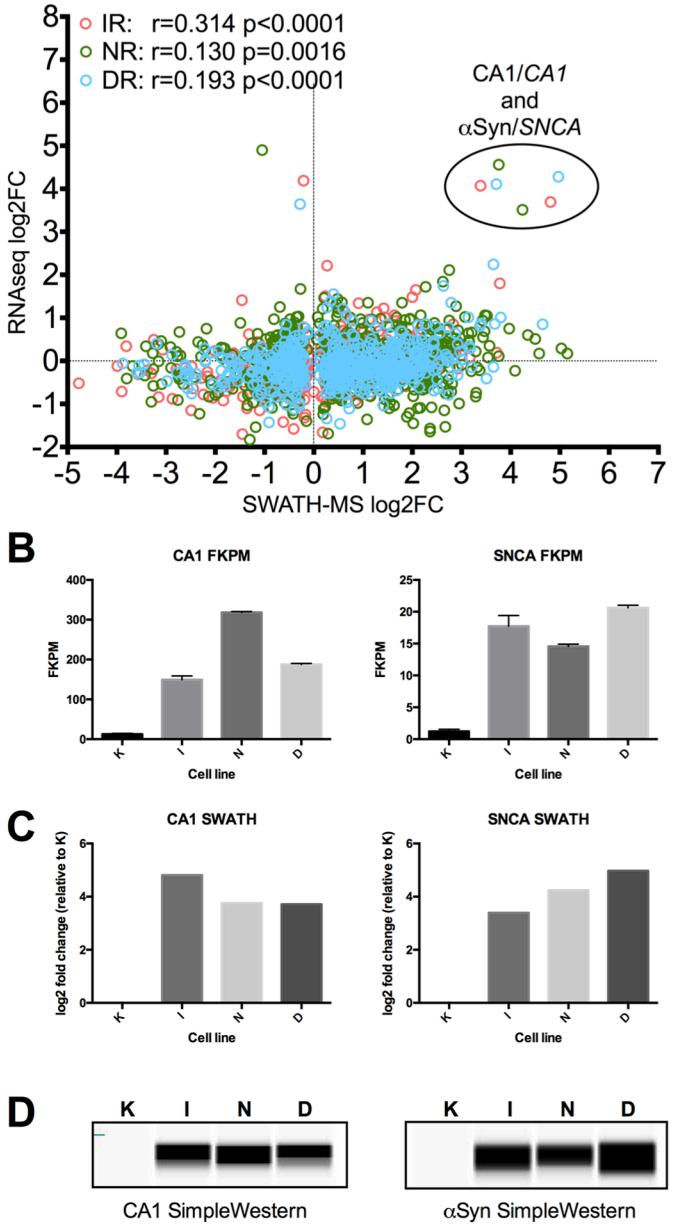

Figure 3. Correlations between mRNA and protein. A) Relationship between mRNA and protein log2 fold change levels from RNAseq and SWATH-MS. IR = imatinib resistant, NR = nilotinib resistant, DR = dasatinib resistant. B) FKPM values plotted for selected gene transcripts showing upregulation at both mRNA and protein levels: CA1 and SNCA (-Synuclein). Error bars represent SEM for three replicate sequencing runs. K = control K562 cells, I = imatinib resistant, N = nilotinib resistant, D = dasatinib resistant. C) SWATH-MS quantitation values from the OneOmics workflow plotted as log2 fold change for resistant lines relative to K, with unchanged K column shown for reference. D) ProteinSimple SimpleWestern chemiluminescence pseudo-blots showing immunodetection of these three proteins. Full SimpleWestern traces and pseudo-blot images available in the Supporting Information.

SWATH-MS results suggesting that post-transcriptional or translational regulation may be an important mechanism in TKI resistance and highlight the importance of matched, protein-level analysis in the study of TKI resistance.

We identified two proteins with large difference of expression at both the mRNA and protein level in all of the resistant samples: carbonic anhydrase 1 (CA1) and α-synuclein (αSyn) (Fig. 3B-C). CA1 is an enzyme that aids in maintaining pH balance both intra- and extracellularly in many systems, and participates in H+/lactate co-transport. Given the requirement for increased carbonic anhydrase activity for cells' adaptation to increased lactate levels in response to high rates of glycolysis,[25,27,28], its upregulation in these cell lines may be related to

metabolic changes arising from mitochondrial dysfunction suggested by IPA (Fig. S4). A role for αSyn in K562 cells has not been previously described; this protein has been described primarily in the setting of Parkinson's disease. However, αSyn interacts with the mitochondrial membrane and is required for mitochondrial fission in response to mitochondrial stress,[29] and plays a role in mitochondrial membrane depolarization (and thus might affect ROS generation)[30,31] implicating a role for this protein in the metabolic alterations detected in the transcriptional analysis. Additionally, αSyn upregulation has been observed in myelodysplastic syndrome and megakaryoblastic leukemias,[32] and given that myeloid progenitor cells give rise to megakaryocytes[33] it is possible that αSyn induction in these cell lines may be related to functional changes in the differentiation state of the resistant cells. αSyn is also associated with extracellular vesicle release from platelets[34] (which arise from the megakaryocyte lineage), however examination of media from cultures of the K562 and resistant cell lines showed no significant increase in exosome secretion in the drug resistant cells relative to the control cells (Fig. S6).

Metabolic reprogramming in TKI resistance: increased dependence on glycolysis and shunting through the pentose phosphate pathway

Our integrated proteomic and transcriptional data suggest that metabolic reprogramming may be an important mechanism of survival in TKI resistant cells. To test this possibility, we performed a ^{13}C-labeled glucose feeding experiment to compare glucose metabolism in IR cells relative to TKI sensitive cells. The cells were passaged into media containing 6-^{13}C-labeled glucose and allowed to grow for 12.5 hours. After this treatment, the metabolites were harvested and

analyzed to study the differences in relative abundance of a panel of metabolites. IR cells showed a consistent and significant increase of relative abundance of glycolysis and pentose phosphate pathway (PPP) metabolites in comparison to the parental line (Figure 4).

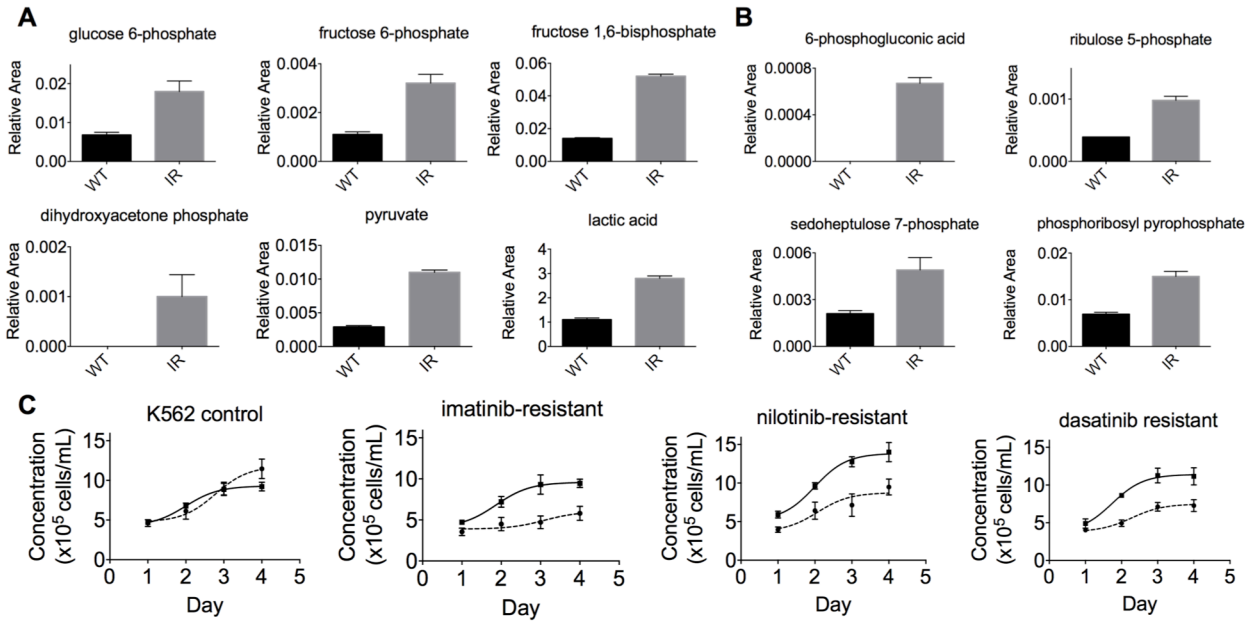

Figure 4. Metabolite profiling and glucose dependence. Metabolite profiling via labeled glucose feeding, comparing "WT" (parental control) with imatinib-resistant (IR). (A) Comparisons for six metabolites involved in the glycolysis pathway of energy production; (B) Comparisons for four metabolites involved in the pentose phosphate pathway (PPP) or, in the case of phosphoribosyl pyrophosphate, synthesized downstream from the PPP intermediate ribulose 5-phosphate. Values are expressed as Relative Area (x-axis) compared to internal standard. Error bars represent standard error of the mean for three technical replicates. (C) Cell growth curves for untreated control (DMSO only), imatinib-resistant, nilotinib-resistant and dasatinib-resistant cells. Cells were grown in duplicate in either glucose-containing (solid lines) or galactose-containing (dashed lines) media for a total of four passages over 16 days. Growth curves for each set of four days after a passage from both duplicates were averaged, and error bars represent standard error of the mean (SEM).

As for many cancers, K562 cells exhibit increased glycolytic activity (relative to non-leukemia cells), commonly known as the Warburg effect.[35,36] Prior evidence from the literature suggests that this is initially suppressed by imatinib exposure (creating the "reverse Warburg effect", in which metabolism in cancer cells shifts away from glycolysis).[35,36] Those studies showed that

glucose uptake and lactate production (by glycolysis) were suppressed and mitochondrial oxidative phosphorylation through the citric acid cycle was enhanced by imatinib treatment. In other words, imatinib treatment of TKI-sensitive K562 cells leads to a shift of metabolism towards that of a non-malignant cell. Our data reveal that longer-term IR cells reverse this effect: these cells display elevated levels of metabolites generated by glycolysis (Figure 4A) and PPP (Figure 4B). These data suggest that imatinib resistance is associated with a reversion to increased glycolysis, using glycolysis to an even higher degree than observed in untreated K562 cells. Accordingly, citric acid cycle intermediates, such as α-ketoglutarate, were either not changed or slightly decreased (Supplemental folder "Metabolite Profiling.zip"). Furthermore, the proportion of G6P containing all six ^{13}C-labeled carbons was higher in the IR than in the control cells (Supplemental folder "Metabolite Profiling.zip"), indicating that the resistant cells more readily take up glucose and have reversed the suppression of glucose uptake that has been reported with imatinib exposure in sensitive cells.

The relative abundance and nearly comprehensive ^{13}C-labeling of metabolites in the PPP in IR cells (Figure 4B) also suggests that the resistant cells processed the labeled glucose rapidly through that pathway as well. Activation of the PPP has previously been identified in the cellular redox response.[37] Separately, it also has been associated with decreased pyruvate kinase (PKM) activity[38] which causes accumulation of phosphoenolpyruvate (PEP), which in turn inhibits triosephosphate isomerase (TPI). TPI is a glycolytic enzyme that interconverts dihydroxyacetone phosphate (DHAP) to glyceraldehyde-3-phosphate, and its inhibition would lead to accumulation of DHAP and absence of glyceraldehyde-3-phosphate. While we did not detect increased PEP levels in IR cells, we did see a marked increase in DHAP levels (from none detected in control

cells to a clearly detectable level in the IR cells, Figure 3A) and did not detect any glyceraldehyde-3-phosphate (in either cell type), consistent with TPI inhibition. Therefore, these ^{13}C-labeling experiments also suggest increased PPP activity in IR cells. Together, these data confirm our transcriptomic and proteomic findings and demonstrate that TKI-resistance is associated with metabolic reprogramming towards reliance on glycolytic metabolism and a shift into the pentose phosphate pathway. Interestingly, these data show that TKI resistance is associated with the reversion of the metabolic changes associated with TKI treatment in sensitive cells. This shift in metabolism has been associated with a variety of malignant phenotypes in cancer cells, including drug resistance.[39]

Next, we tested whether TKI-resistant cells were glycolysis-dependent and defective in oxidative phosphorylation. Cells that are grown in high glucose are known to suppress oxidative phosphorylation and use glycolysis through a phenomenon known as the Crabtree effect.[40] When switched to galactose-containing medium, cells that are competent for oxidative phosphorylation adapt quickly and use galactose as a more efficient energy source through that pathway; cells with defects in galactose metabolism or intrinsic downregulation of oxidative phosphorylation grow slowly or not at all since they rely heavily on glycolysis (which is extremely inefficient with galactose) and are unable to adapt to galactose metabolism through oxidative phosphorylation.[41] Pathway analysis of the protein expression data detected downregulation of pathways that are required for metabolism of galactose via conversion to a UDP-galactose intermediate,[42] including proteins responsible for uridine-5'-phosphate biosynthesis and pyrimidine ribonucleotide de novo biosynthesis (Figure S4). These analyses suggested that the TKI resistant cells would not be competent for galactose metabolism. To test this pathway in

TKI resistance cells, we compared the growth of IR, NR and DR cells in glucose- or galactose-containing medium. While the control cells grew equally well in both media, the TKI resistance cells exhibited a marked decrease in growth rate in galactose (Figure 4C), indicating that the TKI resistant cell lines are unable to efficiently switch between glycolysis and oxidative phosphorylation: they rely on glycolysis and are unable to effectively use galactose for oxidative phosphorylation metabolism. These data demonstrate the pan-TKI resistance is associated with metabolic reprogramming that renders these cells reliant on glycolysis. These data imply that pharmocological interventions that target this effect may be effective in preventing the development of TKI resistance.

Discussion

This study used transcriptomic, proteomic and metabolite profiling of *in vitro* models to broadly evaluate potential mechanisms of TKI resistance in CML. Overall, the gene expression and protein level data from our study suggest that K562 CML cells adapt at multiple levels to grow in the presence of the three commonly used kinase inhibitor drugs, but that metabolic changes underlie many aspects of these levels. Several markers previously found in clinical and animal model-based studies of TKI resistance were observed suggesting that this model does recapitulate well-validated features of TKI-resistance. These features included MDR1/ABCB1,[20] the β-catenin/CD44 pathway,[22] and Axl kinase.[24,43] We also observed features of metabolically-related resistance mechanisms, including apparent induction of hypoxia signaling and PI3K signaling (observed by GSEA and Ingenuity Pathway Analysis), enrichment of proteins related to myo-inositol biosynthesis (part of the pentose phosphate pathway), upregulation of CA1

(indicative of increased need for management of lactate in the cell), as well as the fatty acid transporter CD36, a metabolism-related protein that previously had only been found in TKI resistant CML cells residing in an adipose niche *in vivo*, and a fatty acid binding protein FABP5 (family member of FABP4, which was part of the CD36-related mechanism).[21] The observations of MYC, HIF1 and PI3K pathways is consistent with what is known about tumor metabolic reprogramming and drug resistance,[44] including in BcrAbl-dependent cells,[11] providing further support for the likelihood that these cells have undergone changes to their metabolism in order to evade cell death in the presence of these TKIs.[9] While there are many caveats to using such a model, including the lack of bone marrow niche or other relevant *in vivo* microenvironment, and the differences in dosages present in suspension culture vs. the drug concentration fluctuations and gradients that would be present *in vivo*, this collection of literature-corroborated observations also suggests that despite the limitations of *in vitro* culture of long-established cell lines, these models provide a reasonable degree of relevance to the systems they are intended to mimic. Based on that, the multi-omic changes reported in this work should be of value for considering potential alternative therapeutic mechanisms to pursue for TKI resistant CML.

Metabolic reprogramming as a general drug resistance strategy for K562 CML cells

Multi-drug resistance through metabolic reprogramming and imbalance of the redox equilibrium is increasingly being recognized as an important consideration in chemotherapy for leukemias.[45,46] While TKIs have been very successful in managing CML for about 70-80% of patients, non-response and/or resistance are still significant problems. Drugs such as ponatinib have been developed to address the most common BcrAbl mutations, but these do not solve the problems of

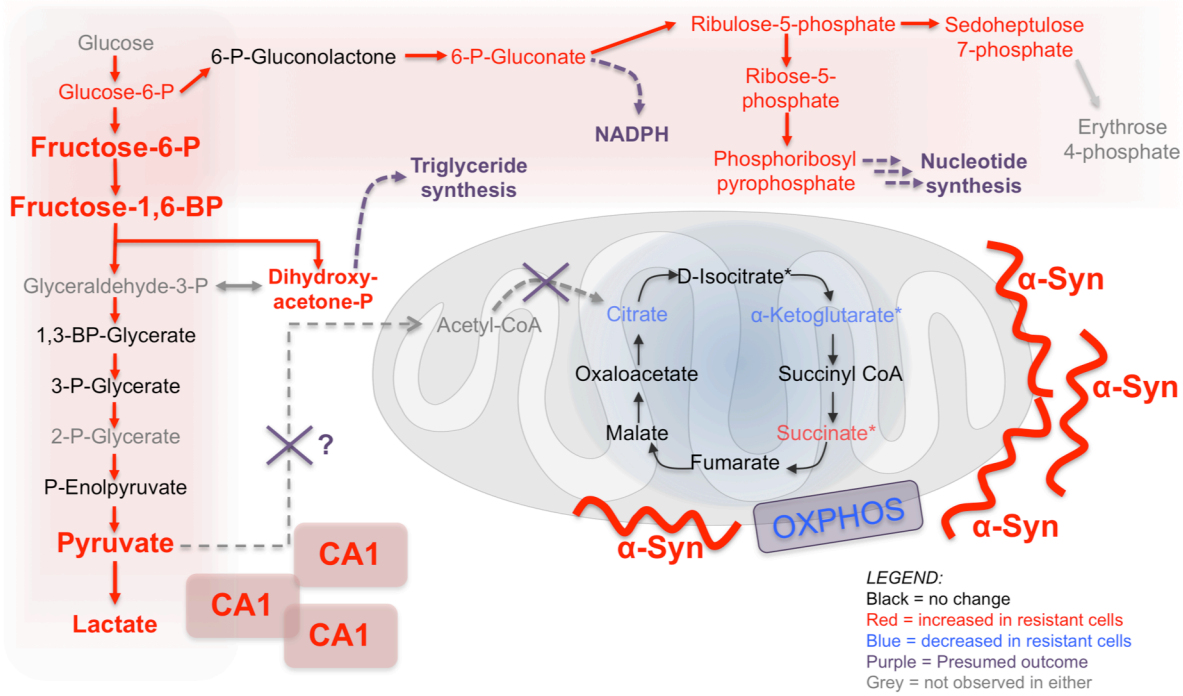

Figure 5. Functional markers of metabolic adaptation in TKI resistant cells. Pan-TKI resistant K562 cells exhibit increased glycolysis and PPP metabolism, with alternate use of dihydroxyacetone-phosphate (presumably re-routed for triglyceride synthesis) and a disconnection of the glycolysis-citric acid cycle cross-talk that is normally mediated through pyruvate. Carbonic anhydrase 1 is upregulated, likely to help buffer excess lactic acid from the increased glycolysis rate, and α-synuclein is upregulated, perhaps to modulate mitochondrial membrane polarization and mitochondrial stress related to the metabolic alterations.

metabolic and redox-related multi-drug resistance. Finding ways to combat more general forms of resistance could have broad utility for off-target TKI resistance in CML and other cancers. Our studies identified these types of metabolic reprogramming and redox features associated with resistance to all three commonly used TKIs, imatinib, nilotinib and dasatinib, indicating that they could play a role in multi-drug resistance in CML.

In particular, the upregulation of CA1 and αSyn could be mechanistically linked markers of metabolic dysregulation in TKI resistance (Figure 5). CA1 is important for buffering cells in the presence of increased lactate concentrations, which result from increased flux through glycolytic pathways. αSyn is involved in mitochondrial dysfunction and handling increased ROS, both of

which are related to metabolism and redox balance in the cell.[30,31,47,48] CA1 and αSyn upregulation in these TKI resistant CML cell models could thus be part of a protective response to metabolic shifts, enabling the cells to better manage the increased lactate and ROS and avoid apoptosis. Although αSyn has been observed in certain cell lines (but not in K562) in a small study looking at synucleins in hematological malignancies,[32] to our knowledge it has not previously been linked to metabolic reprogramming or drug resistance in leukemias. Ultimately, these metabolic adaptations seem to be relatively independent of the specific kinases or cancer type,[49,50,51] and are not consistent with recently proposed models in which OXPHOS (and not the apparent lack of ability to adapt to use OXPHOS, as in our case) is a marker of non-response to chemotherapies.[46,52,53] The mechanisms reported in our work identify mechanisms of resistance in TKI-treated CML cases where no *BCR-ABL1* mutations are observed. Further work is ongoing with these resistant model systems to investigate opportunities to block key metabolic processes that could prevent resistance or resensitize cells to TKIs.

Acknowledgements

We thank the University of Minnesota Genomics Center for next generation sequencing data collection and Juan Abrahante (UMII) for assistance with RNAseq data analysis, and the University of Minnesota Center for Mass Spectrometry and Proteomics, Stephen Tate and Christie Hunter (SCIEX) for assistance with SWATH-MS data collection and analysis. This work was supported by the National Institutes of Health/National Cancer Institute (R01CA182546 and R33CA183671 to LLP). LJM was supported on the UMN Cancer Biology Training Grant (T32 CA009138) and the UMN Physical Sciences Oncology Center grant (U54CA210190).

References cited

1. Druker BJ, O'Brien SG, Cortes J, Radich J. Chronic myelogenous leukemia. *Hematology Am Soc Hematol Educ Program*. 2002:111-135.
2. Sawyers CL. Perspective: combined forces. *Nature*. 2013;498(7455):S7.
3. White D, Saunders V, Grigg A, et al. Measurement of in vivo BCR-ABL kinase inhibition to monitor imatinib-induced target blockade and predict response in chronic myeloid leukemia. *J Clin Oncol*. 2007;25(28):4445-4451.
4. Jabbour EJ, Cortes JE, Kantarjian HM. Resistance to tyrosine kinase inhibition therapy for chronic myelogenous leukemia: a clinical perspective and emerging treatment options. *Clin Lymphoma Myeloma Leuk*. 2013;13(5):515-529.
5. Garg RJ, Kantarjian H, O'Brien S, et al. The use of nilotinib or dasatinib after failure to 2 prior tyrosine kinase inhibitors: long-term follow-up. *Blood*. 2009;114(20):4361-4368.
6. Shah NP, Rousselot P, Schiffer C, et al. Dasatinib in imatinib-resistant or -intolerant chronic-phase, chronic myeloid leukemia patients: 7-year follow-up of study CA180-034. *Am J Hematol*. 2016;91(9):869-874.
7. Cooper MJ, Cox NJ, Zimmerman EI, et al. Application of multiplexed kinase inhibitor beads to study kinome adaptations in drug-resistant leukemia. *PLoS One*. 2013;8(6):e66755.
8. Graves LM, Duncan JS, Whittle MC, Johnson GL. The dynamic nature of the kinome. *Biochem J*. 2013;450(1):1-8.
9. Tarrado-Castellarnau M, de Atauri P, Cascante M. Oncogenic regulation of tumor metabolic reprogramming. *Oncotarget*. 2016;7(38):62726-62753.
10. Herranz D, Ambesi-Impiombato A, Sudderth J, et al. Metabolic reprogramming induces resistance to anti-NOTCH1 therapies in T cell acute lymphoblastic leukemia. *Nat Med*. 2015;21(10):1182-1189.
11. Zhao F, Mancuso A, Bui TV, et al. Imatinib resistance associated with BCR-ABL upregulation is dependent on HIF-1alpha-induced metabolic reprograming. *Oncogene*. 2010;29(20):2962-2972.
12. Edfors F, Danielsson F, Hallstrom BM, et al. Gene-specific correlation of RNA and protein levels in human cells and tissues. *Mol Syst Biol*. 2016;12(10):883.
13. Ouellette SB, Noel BM, Parker LL. A Cell-Based Assay for Measuring Endogenous BcrAbl Kinase Activity and Inhibitor Resistance. *PLoS One*. 2016;11(9):e0161748.
14. Trapnell C, Williams BA, Pertea G, et al. Transcript assembly and quantification by RNA-Seq reveals unannotated transcripts and isoform switching during cell differentiation. *Nat Biotechnol*. 2010;28(5):511-515.
15. McPherson A, Hormozdiari F, Zayed A, et al. deFuse: an algorithm for gene fusion discovery in tumor RNA-Seq data. *PLoS Comput Biol*. 2011;7(5):e1001138.
16. Kumarakulasingham M, Rooney PH, Dundas SR, et al. Cytochrome p450 profile of colorectal cancer: identification of markers of prognosis. *Clin Cancer Res*. 2005;11(10):3758-3765.
17. Gillet LC, Navarro P, Tate S, et al. Targeted data extraction of the MS/MS spectra generated by data-independent acquisition: a new concept for consistent and accurate proteome analysis. *Mol Cell Proteomics*. 2012;11(6):O111 016717.

18. Levin JZ, Berger MF, Adiconis X, et al. Targeted next-generation sequencing of a cancer transcriptome enhances detection of sequence variants and novel fusion transcripts. *Genome Biol*. 2009;10(10):R115.
19. Zhou MH, Yang QM. NUP214 fusion genes in acute leukemia (Review). *Oncol Lett*. 2014;8(3):959-962.
20. Eadie LN, Dang P, Saunders VA, et al. The clinical significance of ABCB1 overexpression in predicting outcome of CML patients undergoing first-line imatinib treatment. *Leukemia*. 2017;31(1):75-82.
21. Ye H, Adane B, Khan N, et al. Leukemic Stem Cells Evade Chemotherapy by Metabolic Adaptation to an Adipose Tissue Niche. *Cell Stem Cell*. 2016;19(1):23-37.
22. Zhou H, Mak PY, Mu H, et al. Combined inhibition of beta-catenin and Bcr-Abl synergistically targets tyrosine kinase inhibitor-resistant blast crisis chronic myeloid leukemia blasts and progenitors in vitro and in vivo. *Leukemia*. 2017;31(10):2065-2074.
23. Grosso S, Puissant A, Dufies M, et al. Gene expression profiling of imatinib and PD166326-resistant CML cell lines identifies Fyn as a gene associated with resistance to BCR-ABL inhibitors. *Mol Cancer Ther*. 2009;8(7):1924-1933.
24. Dufies M, Jacquel A, Belhacene N, et al. Mechanisms of AXL overexpression and function in Imatinib-resistant chronic myeloid leukemia cells. *Oncotarget*. 2011;2(11):874-885.
25. Martinez-Outschoorn UE, Peiris-Pages M, Pestell RG, Sotgia F, Lisanti MP. Cancer metabolism: a therapeutic perspective. *Nat Rev Clin Oncol*. 2017;14(1):11-31.
26. Boulahbel H, Duran RV, Gottlieb E. Prolyl hydroxylases as regulators of cell metabolism. *Biochem Soc Trans*. 2009;37(Pt 1):291-294.
27. Hulikova A, Aveyard N, Harris AL, Vaughan-Jones RD, Swietach P. Intracellular carbonic anhydrase activity sensitizes cancer cell pH signaling to dynamic changes in CO2 partial pressure. *J Biol Chem*. 2014;289(37):25418-25430.
28. Swietach P, Vaughan-Jones RD, Harris AL, Hulikova A. The chemistry, physiology and pathology of pH in cancer. *Philos Trans R Soc Lond B Biol Sci*. 2014;369(1638):20130099.
29. Norris KL, Hao R, Chen LF, et al. Convergence of Parkin, PINK1, and alpha-Synuclein on Stress-induced Mitochondrial Morphological Remodeling. *J Biol Chem*. 2015;290(22):13862-13874.
30. Rostovtseva TK, Gurnev PA, Protchenko O, et al. alpha-Synuclein Shows High Affinity Interaction with Voltage-dependent Anion Channel, Suggesting Mechanisms of Mitochondrial Regulation and Toxicity in Parkinson Disease. *J Biol Chem*. 2015;290(30):18467-18477.
31. Bir A, Sen O, Anand S, et al. alpha-Synuclein-induced mitochondrial dysfunction in isolated preparation and intact cells: implications in the pathogenesis of Parkinson's disease. *J Neurochem*. 2014;131(6):868-877.
32. Maitta RW, Wolgast LR, Wang Q, et al. Alpha- and beta-synucleins are new diagnostic tools for acute erythroid leukemia and acute megakaryoblastic leukemia. *Am J Hematol*. 2011;86(2):230-234.
33. Woolthuis CM, Park CY. Hematopoietic stem/progenitor cell commitment to the megakaryocyte lineage. *Blood*. 2016;127(10):1242-1248.
34. Pienimaeki-Roemer A, Kuhlmann K, Bottcher A, et al. Lipidomic and proteomic characterization of platelet extracellular vesicle subfractions from senescent platelets. *Transfusion*. 2015;55(3):507-521.

35. Gottschalk S, Anderson N, Hainz C, Eckhardt SG, Serkova NJ. Imatinib (STI571)-mediated changes in glucose metabolism in human leukemia BCR-ABL-positive cells. *Clin Cancer Res*. 2004;10(19):6661-6668.
36. Hirao T, Yamaguchi M, Kikuya M, Chibana H, Ito K, Aoki S. Altered intracellular signaling by imatinib increases the anti-cancer effects of tyrosine kinase inhibitors in chronic myelogenous leukemia cells. *Cancer Sci*. 2018;109(1):121-131.
37. Kruger A, Gruning NM, Wamelink MM, et al. The pentose phosphate pathway is a metabolic redox sensor and regulates transcription during the antioxidant response. *Antioxid Redox Signal*. 2011;15(2):311-324.
38. Gruning NM, Rinnerthaler M, Bluemlein K, et al. Pyruvate kinase triggers a metabolic feedback loop that controls redox metabolism in respiring cells. *Cell Metab*. 2011;14(3):415-427.
39. Patra KC, Hay N. The pentose phosphate pathway and cancer. *Trends Biochem Sci*. 2014;39(8):347-354.
40. Ibsen KH. The Crabtree effect: a review. *Cancer Res*. 1961;21:829-841.
41. Robinson BH, Petrova-Benedict R, Buncic JR, Wallace DC. Nonviability of cells with oxidative defects in galactose medium: a screening test for affected patient fibroblasts. *Biochem Med Metab Biol*. 1992;48(2):122-126.
42. Pelley JW. 9 - Minor Carbohydrate Pathways: Ribose, Fructose, and Galactose. Elsevier's Integrated Biochemistry. Philadelphia: Mosby; 2007:73-77.
43. Ben-Batalla I, Erdmann R, Jorgensen H, et al. Axl Blockade by BGB324 Inhibits BCR-ABL Tyrosine Kinase Inhibitor-Sensitive and -Resistant Chronic Myeloid Leukemia. *Clin Cancer Res*. 2017;23(9):2289-2300.
44. Schito L, Semenza GL. Hypoxia-Inducible Factors: Master Regulators of Cancer Progression. *Trends Cancer*. 2016;2(12):758-770.
45. Vidal RS, Quarti J, Rumjanek FD, Rumjanek VM. Metabolic Reprogramming During Multidrug Resistance in Leukemias. *Front Oncol*. 2018;8:90.
46. Kim HK, Noh YH, Nilius B, et al. Current and upcoming mitochondrial targets for cancer therapy. *Semin Cancer Biol*. 2017;47:154-167.
47. Samudio I, Fiegl M, Andreeff M. Mitochondrial uncoupling and the Warburg effect: molecular basis for the reprogramming of cancer cell metabolism. *Cancer Res*. 2009;69(6):2163-2166.
48. Sack MN. Mitochondrial depolarization and the role of uncoupling proteins in ischemia tolerance. *Cardiovasc Res*. 2006;72(2):210-219.
49. Amoedo ND, Punzi G, Obre E, et al. AGC1/2, the mitochondrial aspartate-glutamate carriers. *Biochim Biophys Acta*. 2016;1863(10):2394-2412.
50. Strickland M, Stoll EA. Metabolic Reprogramming in Glioma. *Front Cell Dev Biol*. 2017;5:43.
51. Allegra A, Innao V, Gerace D, Bianco O, Musolino C. The metabolomic signature of hematologic malignancies. *Leuk Res*. 2016;49:22-35.
52. Bosc C, Selak MA, Sarry JE. Resistance Is Futile: Targeting Mitochondrial Energetics and Metabolism to Overcome Drug Resistance in Cancer Treatment. *Cell Metab*. 2017;26(5):705-707.
53. Farge T, Saland E, de Toni F, et al. Chemotherapy-Resistant Human Acute Myeloid Leukemia Cells Are Not Enriched for Leukemic Stem Cells but Require Oxidative Metabolism. *Cancer Discov*. 2017;7(7):716-735.